Supplementary Materials to accompany

A Tail Does Not Always Make a Difference: Assembly of *cds* Nets from $Co(NCS)_2$ and 1,4-bis(*n*-Alkyloxy)-2,5-bis(3,2′:6′,3′′-terpyridin-4′-yl)benzene Ligands

Simona S. Capomolla, Giacomo Manfroni, Alessandro Prescimone, Edwin C. Constable and Catherine E. Housecroft *

Department of Chemistry, University of Basel, BPR 1096, Mattenstrasse 24a, CH-4058 Basel, Switzerland

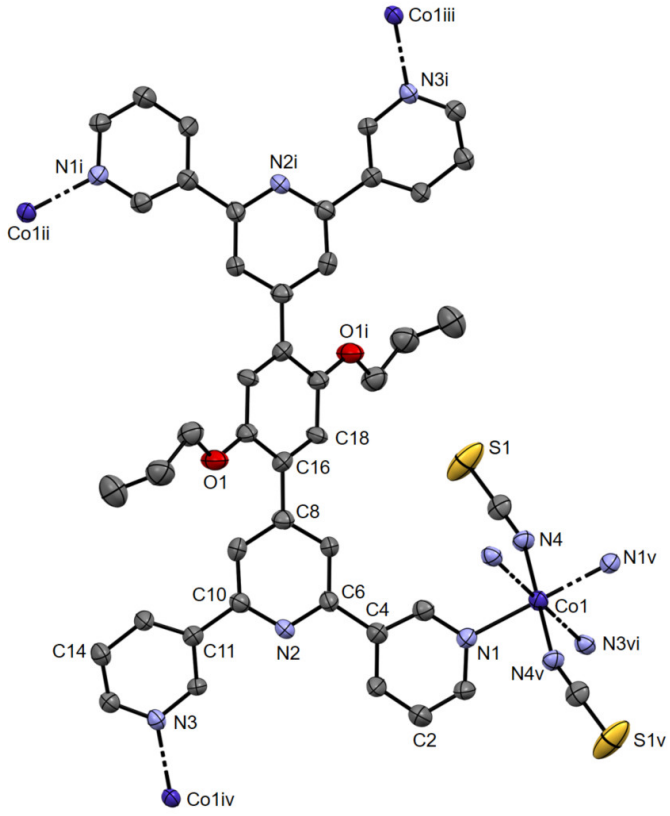

Figure S1. The structure of the asymmetric unit in $[Co(NCS)_2(\mathbf{3})]_n{\cdot}3.5n C_6H_4Cl_2$, with symmetry generated atoms. Hydrogen atoms are omitted for clarity; ellipsoids are plotted at 50% probability level. Symmetry codes: i = –1–*x*, –1–*y*, –1–*z*; ii = 1+*x*, *y*, 1+*z*; iii= –1–*x*, $^1/_2$+*y*, $-^3/_2$–*z*; iv = –2–*x*, $-^1/_2$+*y*, $-^3/_2$–*z*; v = –2–*x*, –1–*y*, –2–*z*; vi= –2–*x*, $^1/_2$+*y*, $-^3/_2$–*z*.

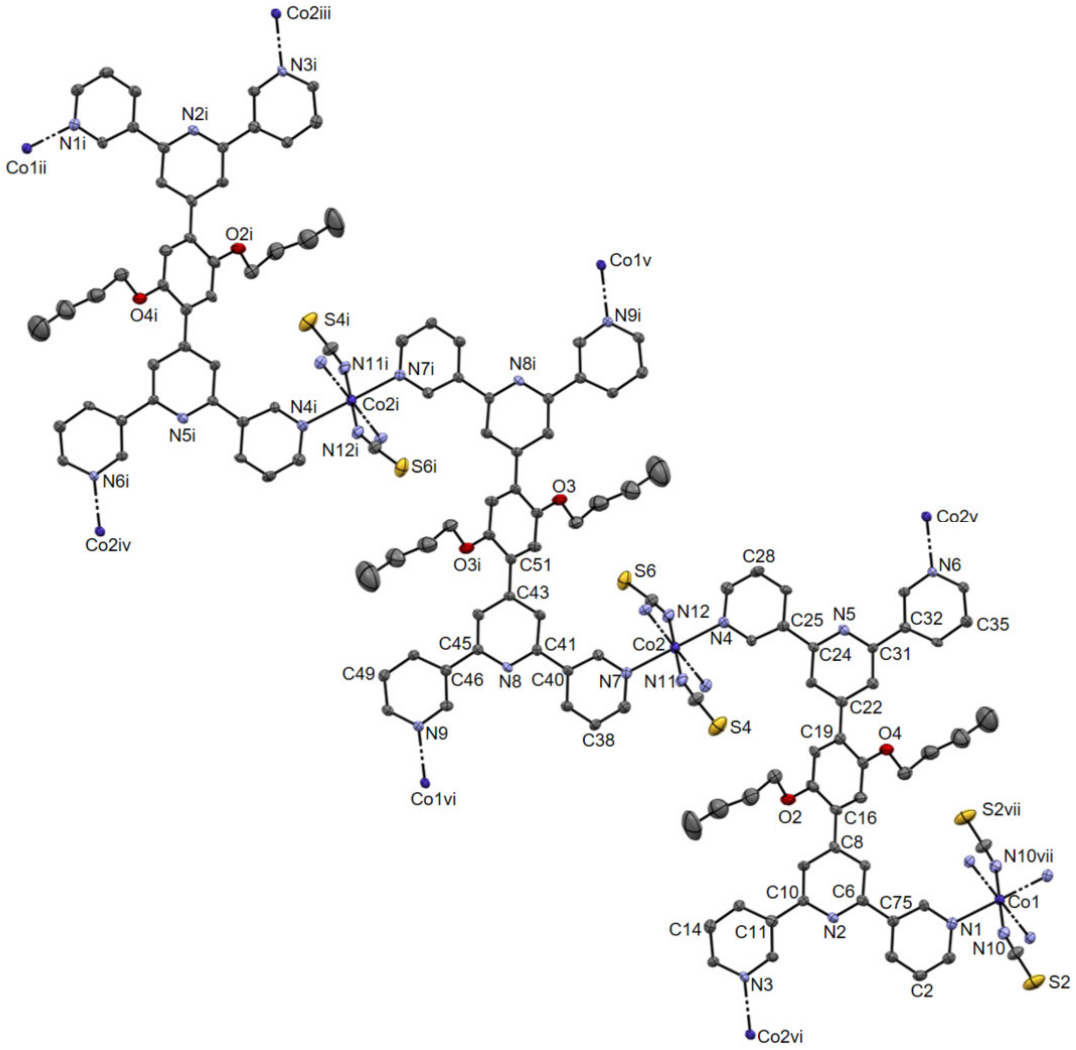

Figure S2. The structure of the asymmetric unit in $[Co(NCS)_2(\mathbf{4})]_n{\cdot}5.5n C_6H_4Cl_2$, with symmetry generated atoms. Hydrogen atoms and solvent molecules are omitted for clarity; ellipsoids are plotted at 50% probability level. Symmetry codes: i = 1–x, 1–y, 2–z; ii = –1+x, y, 1+z; iii = –1+x, $^1/_2$–y, $^1/_2$+z; iv = x, $^1/_2$–y, $^1/_2$+z; v = 1–x, –$^1/_2$+y, $^3/_2$–z; vi = 2–x, $^1/_2$+y, $^3/_2$–z; vii = 2–x, 1–y, 1–z. The sulfur atoms S2, S4 and S6 of the $[NCS]^-$ units are disordered and have been modelled over sites of 50:30:20%, 60:20:20% and 70:30% occupancies, respectively, and only the major occupancy site is shown. The terminal unit in the –OButyl chain on O3 is disordered and has been modelled over sites of 75% and 25% occupancies and only the major occupancy site is shown.

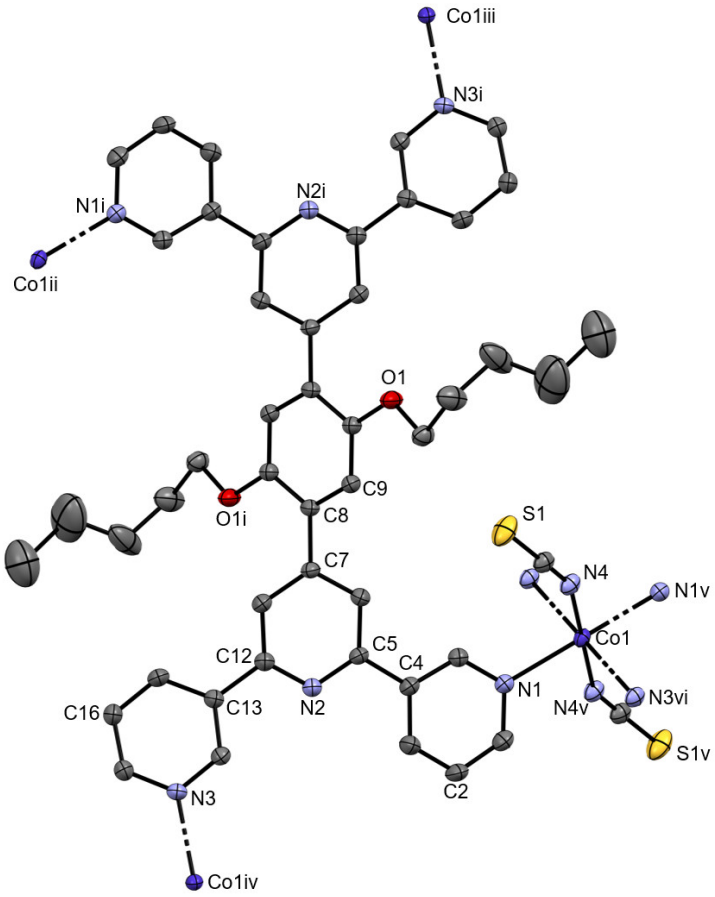

Figure S3. The structure of the asymmetric unit in $[Co(NCS)_2(\mathbf{5})]_n \cdot 4n C_6H_4Cl_2$, with symmetry generated atoms. Hydrogen atoms and solvent molecules are omitted for clarity; ellipsoids are plotted at 50% probability level. Symmetry codes: i = 1–*x*, 1–*y*, 1–*z*; ii = *x*, *y*, 1+*z*; iii = $^1/_2$–*x*, $^1/_2$+*y*, $^1/_2$–*z*; iv = $^3/_2$–*x*, –$^1/_2$ + *y*, $^1/_2$–*z*; v = 1–*x*, 1–*y*, –*z*; vi = $^3/_2$–*x*, ½+*y*, $^1/_2$–*z*.

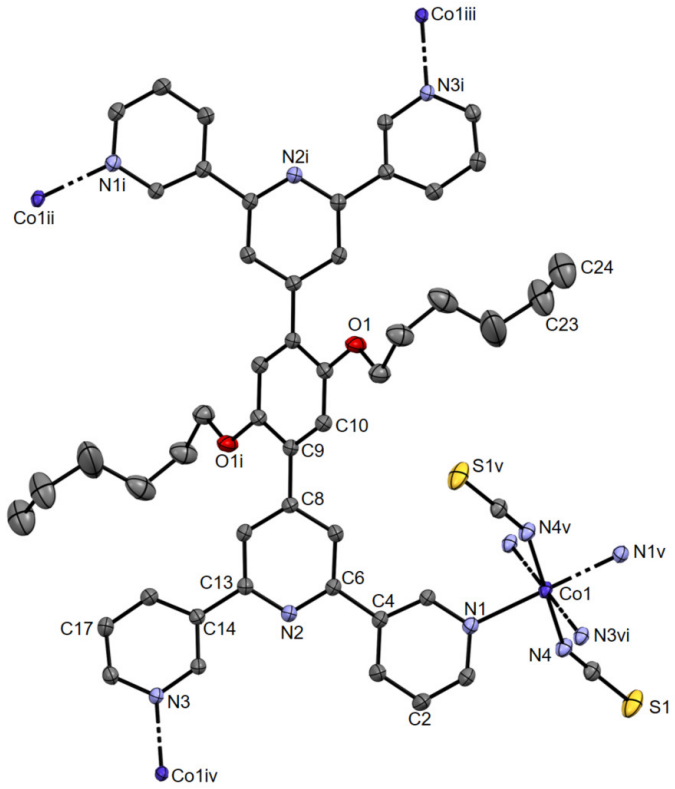

Figure S4. The structure of the asymmetric unit in $[Co(NCS)_2(\mathbf{6})]_n{\cdot}3.8n C_6H_4Cl_2$, with symmetry generated atoms. Hydrogen atoms and solvent molecules are omitted for clarity; ellipsoids are plotted at 50% probability level. Symmetry codes: i = 1–*x*, 1–*y*, 2–*z*; ii = *x*, *y*, 1+*z*; iii = $^1/_2$–*x*, ½+*y*, $^3/_2$–*z*; iv = $^3/_2$–*x*, –$^1/_2$+*y*, $^3/_2$–*z*; v = 1–*x*, 1–*y*, 1–*z*; vi = $^3/_2$–*x*, $^1/_2$+*y*, $^3/_2$–*z*. The terminal units with C23 and C24 in the –OHexyl chain are disordered and have been modelled over sites of 60% and 40% occupancies and only the major one is shown.

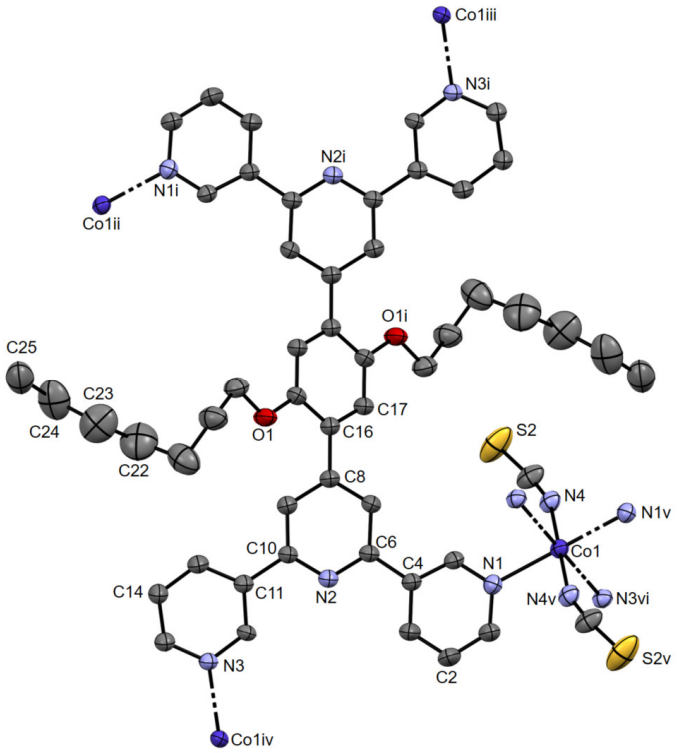

Figure S5. The structure of the asymmetric unit in $[Co(NCS)_2(\mathbf{7})]_n \cdot 3.1n C_6H_4Cl_2$, with symmetry generated atoms. Hydrogen atoms and solvent molecules are omitted for clarity; ellipsoids are plotted at 50% probability level. Symmetry codes: i = 1–*x*, 1–*y*, 1–*z*; ii = *x*, *y*, –1+*z*; iii = $^3/_2$–*x*, $-^1/_2$+*y*, $^3/_2$–*z*; iv = $^1/_2$–*x*, $^1/_2$+*y*, $^3/_2$–*z*; v = 1–*x*, 1–*y*, 2–*z*; vi = $^1/_2$–*x*, $-^1/_2$+*y*, $^3/_2$–*z*. The terminal units with C22, C23, C24 and C25 in the –OHeptyl chain are disordered and have been modelled over sites of 50% and 50% occupancies and only one of the equal occupancy sites is shown. The sulfur S2 of the $[NCS]^-$ unit is disordered and has been modelled over sites of 80% and 20% occupancies and only the major occupancy site is shown.

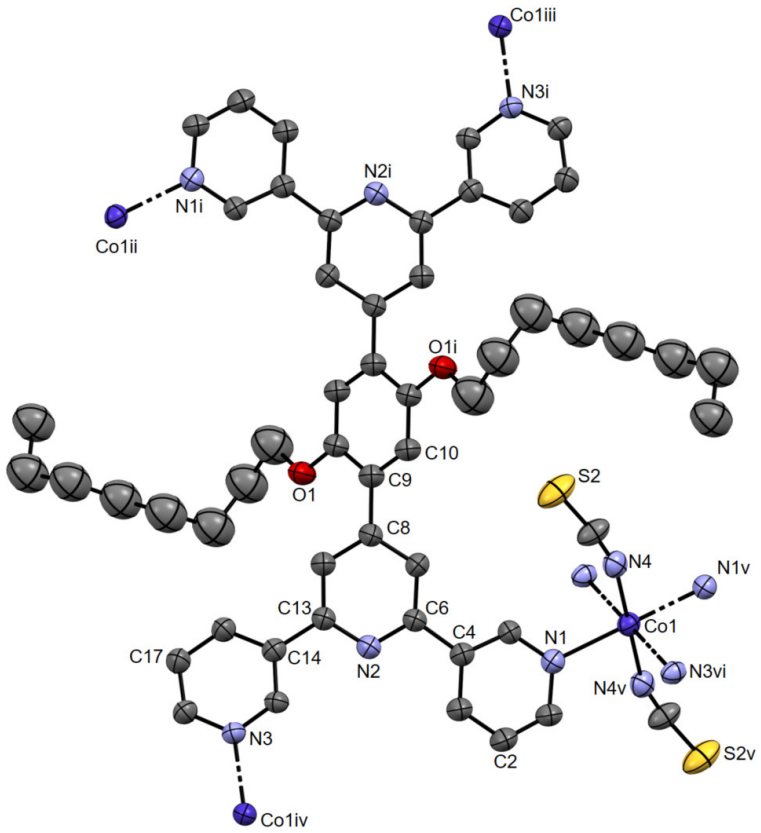

Figure S6. The structure of the asymmetric unit in $[Co(NCS)_2(\mathbf{8})]_n \cdot 1.6n C_6H_4Cl_2 \cdot 2n MeOH$, with symmetry generated atoms. Hydrogen atoms and solvent molecules are omitted for clarity; ellipsoids are plotted at 50% probability level. Symmetry codes: i = –x, 1–y, 1–z; ii = x, y, 1+z; iii = $-^1/_2-x$, $^1/_2+y$, $^1/_2-z$; iv = $^1/_2-x$, $-^1/_2+y$, $^1/_2-z$; v = –x, 1–y, –z; vi = $^1/_2-x$, $^1/_2+y$, $^1/_2-z$. The sulfur atom S2 of the $[NCS]^-$ unit is disordered and has been modelled over sites of 80% and 20% occupancies and only the major occupancy site is shown.

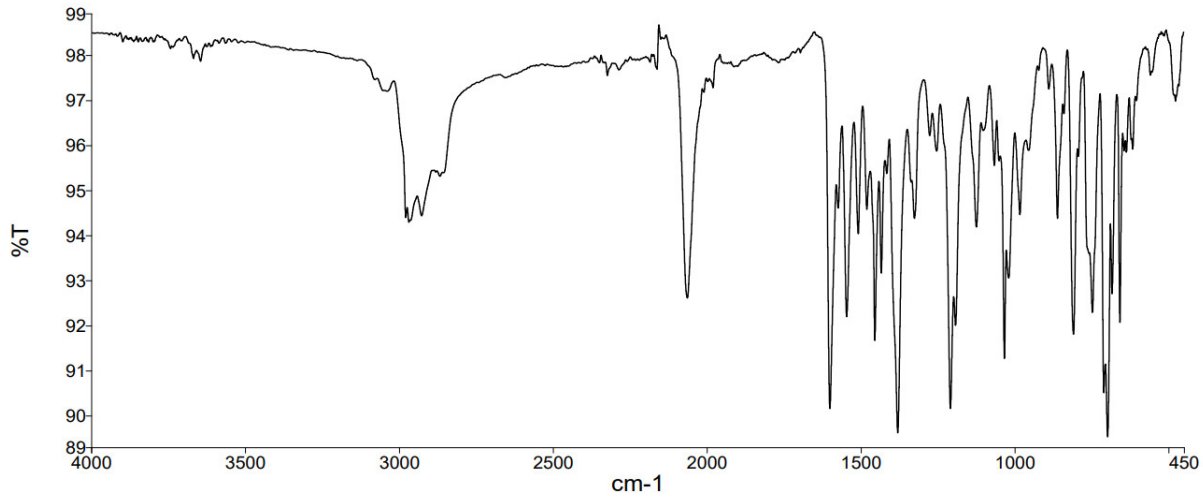

Figure S7. The solid-state FT-IR spectrum of $[Co(NCS)_2(\mathbf{3})]_n \cdot 3.5n C_6H_4Cl_2$.

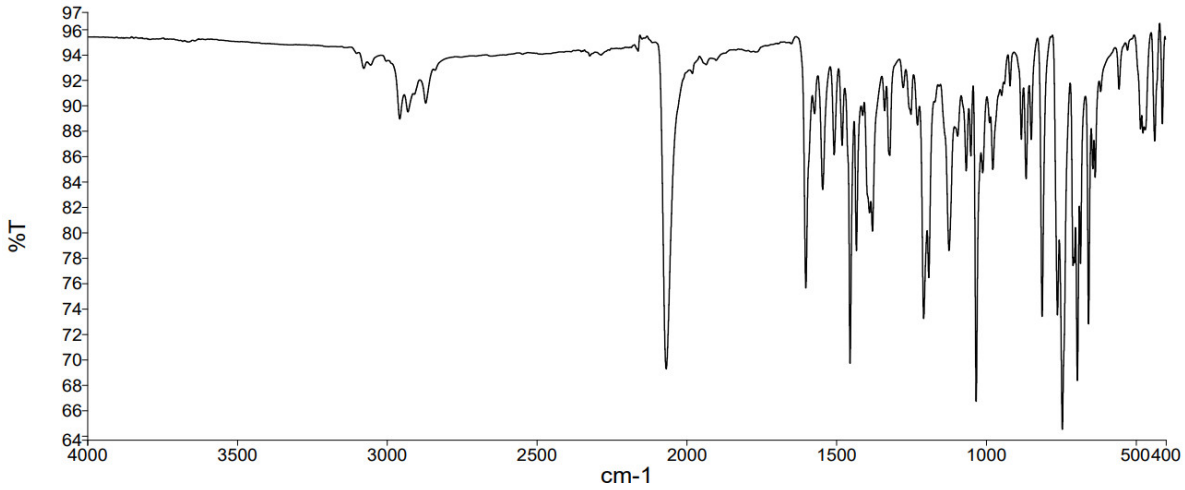

Figure S8. The solid-state FT-IR spectrum of $[Co(NCS)_2(\mathbf{4})]_n \cdot 5.5n C_6H_4Cl_2$.

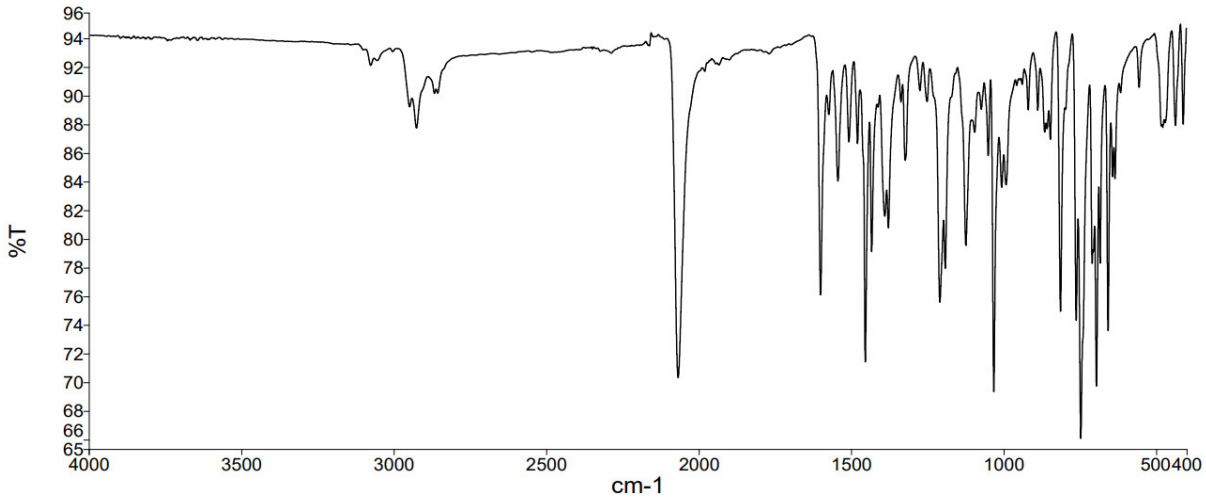

Figure S9. The solid-state FT-IR spectrum of $[Co(NCS)_2(\mathbf{5})]_n \cdot 4n C_6H_4Cl_2$.

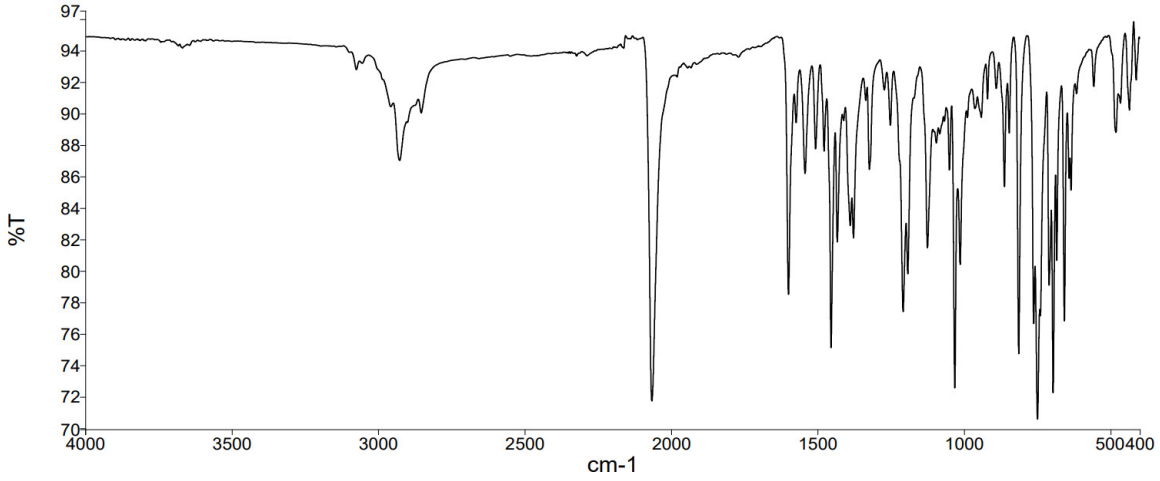

Figure S10. The solid-state FT-IR spectrum of $[Co(NCS)_2(\mathbf{6})]_n \cdot 3.8n C_6H_4Cl_2$.

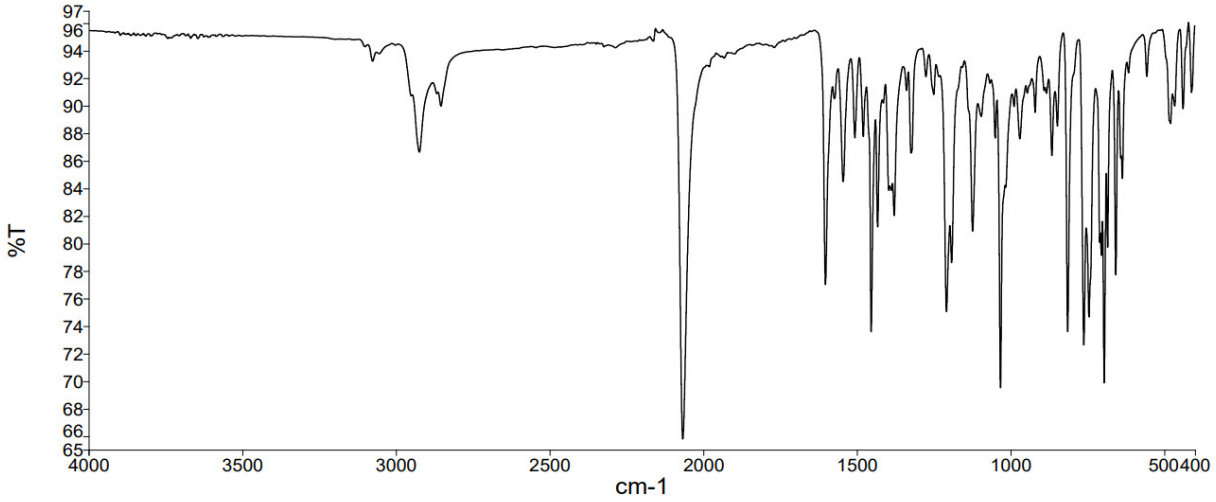

Figure S11. The solid-state FT-IR spectrum of $[Co(NCS)_2(\mathbf{7})]_n \cdot 3.1n C_6H_4Cl_2$.

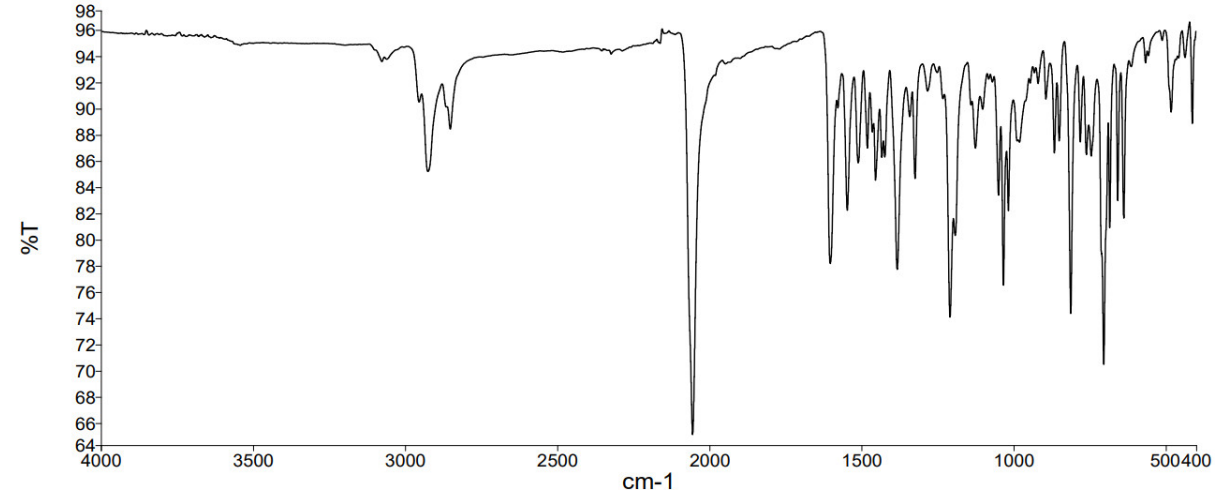

Figure S12. The solid-state FT-IR spectrum of $[Co(NCS)_2(\mathbf{8})]_n \cdot 1.6n C_6H_4Cl_2 \cdot 2n MeOH$.

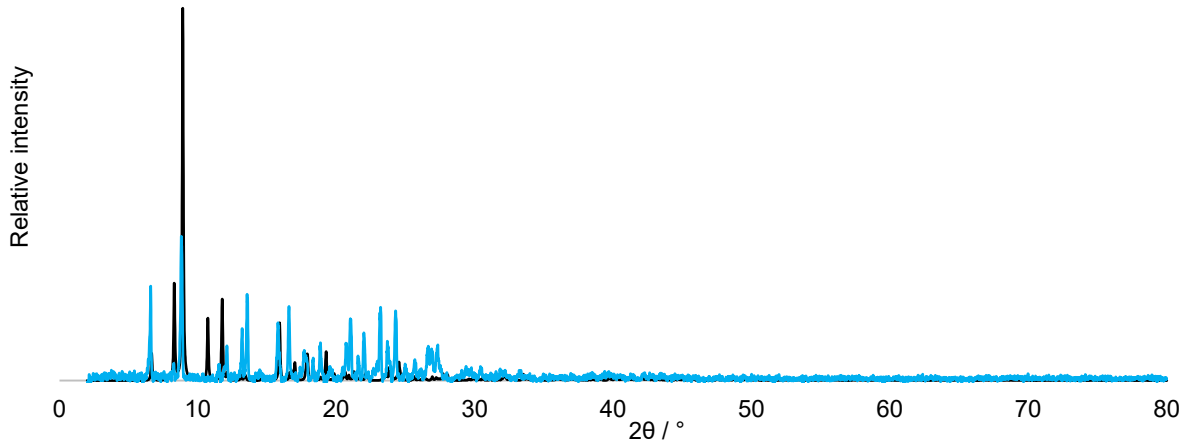

Figure S13. Overlay of the experimental (blue) PXRD (298 K) for the bulk material and that predicted (black) from the single crystal structure (150 K) of $[Co(NCS)_2(\mathbf{3})]_n \cdot 3.5n C_6H_4Cl_2$.

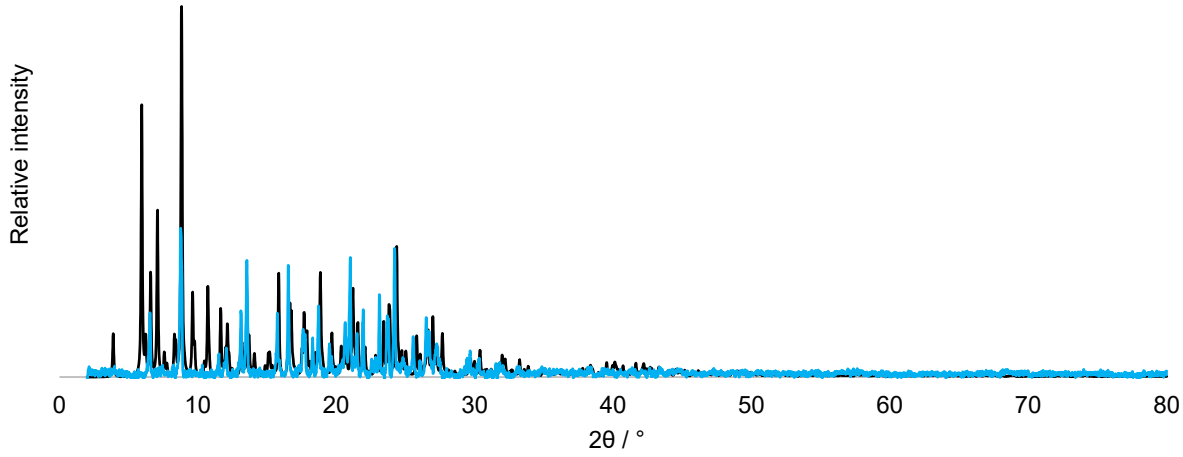

Figure S14. Overlay of the experimental (blue) PXRD (298 K) for the bulk material and that predicted (black) from the single crystal structure (150 K) of $[Co(NCS)_2(\mathbf{4})]_n \cdot 5.5nC_6H_4Cl_2$.

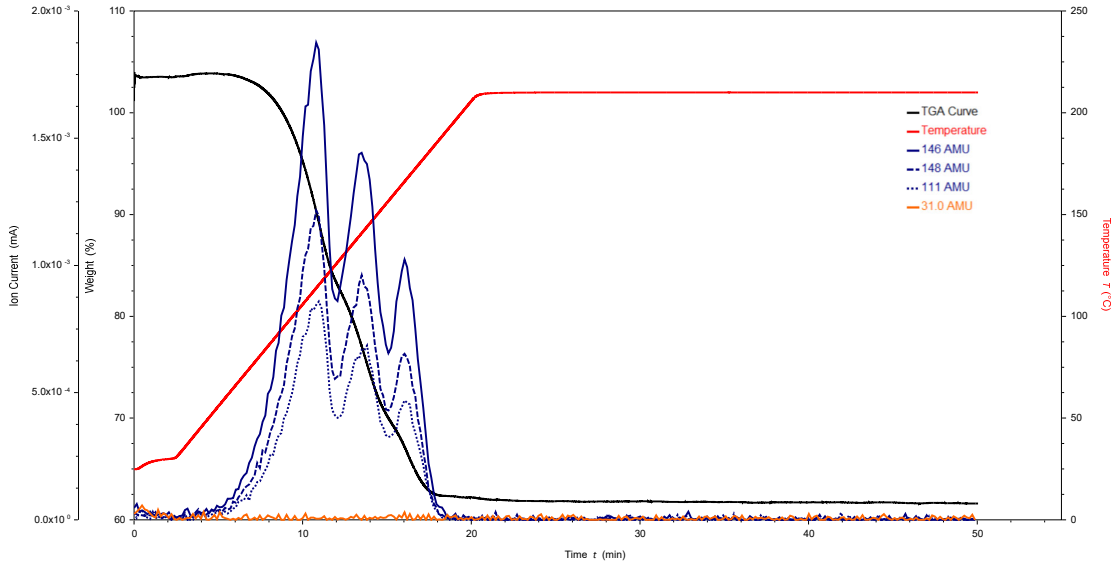

Figure S15. TGA and mass spectrometric traces for the analysis of $[Co(NCS)_2(\mathbf{3})]_n \cdot 3.5nC_6H_4Cl_2$. Red: temperature vs. time; black: weight of sample vs. time; dark blue: mass detection for *m*/*z* 146, 148 and 111; orange: mass detection for *m*/*z* 31.0.

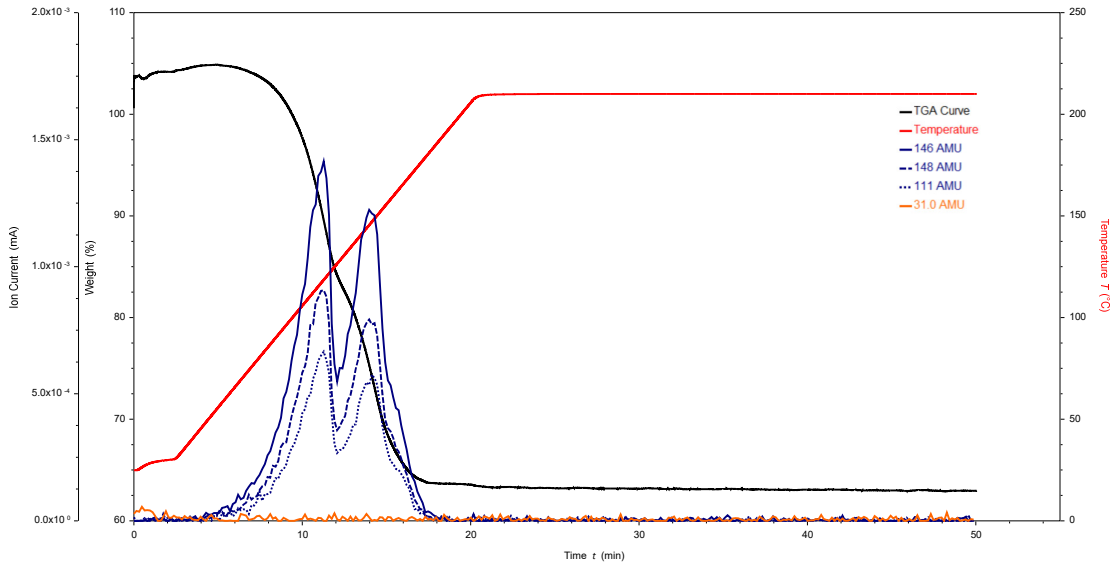

Figure S16.TGA and mass spectrometric traces for the analysis of $[Co(NCS)_2(\mathbf{4})]_n{\cdot}5.5nC_6H_4Cl_2$. Red: temperature vs. time; black: weight of sample vs. time; dark blue: mass detection for *m*/*z* 146, 148 and 111; orange: mass detection for *m*/*z* 31.0.

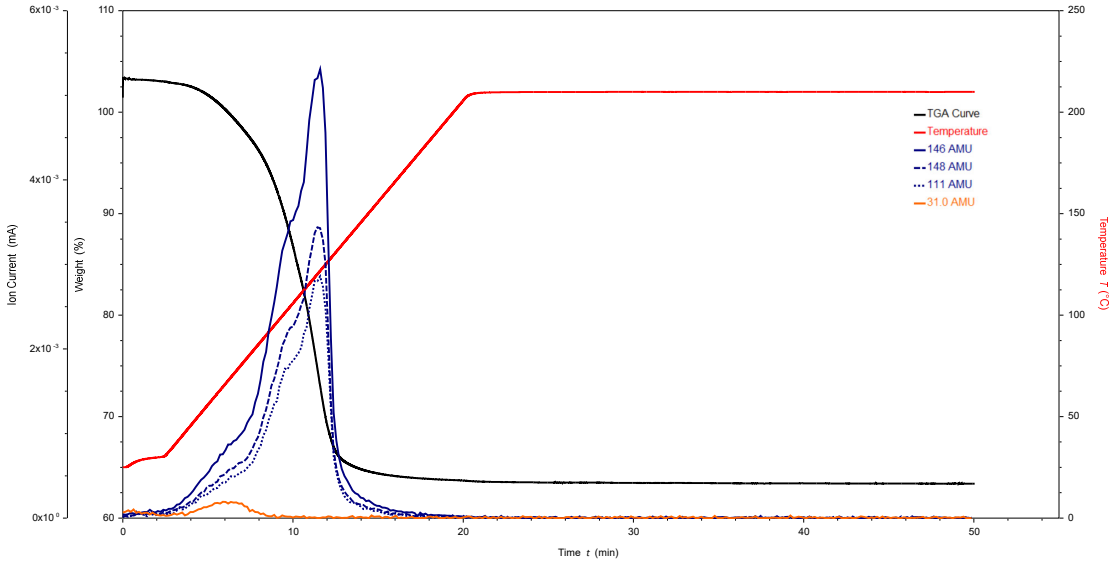

Figure S17. TGA and mass spectrometric traces for the analysis of $[Co(NCS)_2(\mathbf{6})]_n{\cdot}3.8nC_6H_4Cl_2$. Red: temperature vs. time; black: weight of sample vs. time; dark blue: mass detection for *m*/*z* 146, 148 and 111; orange: mass detection for *m*/*z* 31.0.